Advances in Computer, Signals and Systems (2025)
Clausius Scientific Press, Canada

DOI: 10.23977/acss.2025.090412
ISSN 2371-8838 Vol. 9 Num. 4

Improvement of Particle Swarm Algorithm for Multi-objective Planting Scheme Optimization and Empirical Analysis

Yanzhuo Wu, Guangwu Ao*

School of Computer Science and Software Engineering, University of Science and Technology Liaoning, Anshan, 114051, China
**Corresponding Author*

Keywords: Improvement of particle swarm algorithm; Multi-objective optimization; Planting plan; Machine learning; Empirical analysis

Abstract: To address the issues of low resource utilization efficiency and poor multi-objective coordination in traditional planting scheme optimization, by integrating the particle swarm algorithm with machine learning technology, an improved particle swarm algorithm that incorporates adaptive inertia weight, chaotic disturbance mechanism, and Pareto elite retention strategy is proposed. A multi-objective planting scheme optimization model is constructed. Taking a typical agricultural area as the empirical object, multi-dimensional data such as soil, climate, and market are collected. The decision variables such as crop types, planting area, and irrigation strategy are optimized through the improved algorithm. The experimental results show that the convergence speed of the improved algorithm is 32.6% and 21.8% higher than that of the standard PSO and MOPSO algorithms respectively. The optimal planting scheme generated can increase the total crop yield of the region by 15.3%, improve the water resource utilization rate by 28.5%, and increase the economic benefits by 19.7%. This research verifies the effectiveness and superiority of the improved particle swarm algorithm in multi-objective planting optimization, providing a scientific basis and technical support for agricultural modernization planting decisions.

1. Introduction

During the process of agricultural modernization transformation, the optimization of planting systems faces the concurrent demands for resource intensive utilization, capacity enhancement, and ecological sustainable development[1]. Traditional planting schemes mostly rely on empirical decision-making, which have problems such as poor multi-objective coordination and low resource allocation efficiency, and are difficult to adapt to the complex and variable agricultural production scenarios. The multi-objective optimization theory provides an effective paradigm to solve this predicament. The particle swarm algorithm, due to its simple structure and high optimization efficiency, has shown significant application potential in agricultural optimization decision-making[2]. Combined with machine learning technology, it can further enhance the data-driven

capability and prediction accuracy of the optimization model. Therefore, conducting research on multi-objective planting scheme optimization based on the improved particle swarm algorithm is of significant theoretical and practical significance for promoting the transformation of agricultural production from empirical decision-making to intelligent decision-making, and improving the efficiency and comprehensive benefits of agricultural resource utilization[3].

By reviewing the existing research results, it can be seen that multi-objective planting scheme optimization has gradually evolved from traditional linear programming methods to intelligent algorithms [4]. Particle swarm algorithms and genetic algorithms have been widely applied in the optimization research of crop layout, water and fertilizer regulation, etc. At the same time, scholars have proposed improvement directions such as parameter adaptive adjustment and mixed search strategies to address the shortcomings of premature convergence and insufficient solution distribution uniformity of the particle swarm algorithm [5]. The integration of machine learning and optimization algorithms has become an important research paradigm in agricultural data-driven optimization. However, existing research still has obvious gaps [6]. For example, the improvements of the particle swarm algorithm mainly focus on a single defect, have insufficient adaptability to multi-objective collaborative optimization scenarios, have a low coupling degree between the optimization model and the actual planting scenario, and the targetedness and practicality of empirical research need to be strengthened [7]. These problems provide a clear entry point for this study.

2. Methods

2.1 Basic Theory and Supporting Technologies

The Particle Swarm Optimization (PSO) algorithm is inspired by the foraging behavior of bird flocks. It achieves optimization through the collaboration and information sharing among particles in the group. In the standard PSO, each particle represents a potential solution to the optimization problem[8]. It updates its own velocity and position by tracking the individual best solution (pbest) and the global best solution (gbest). The mathematical models are as shown in Equations (1) and (2):

$$\mathbf{v}_{i,d}^{t+1} = \omega \mathbf{v}_{i,d}^{t} + c_1 \mathbf{r}_1 (pbest_{i,d}^{t} - x_{i,d}^{t}) + c_2 \mathbf{r}_2 (gbest_{d}^{t} - x_{i,d}^{t}) \quad (1)$$

In Equation (1), v represents the velocity of the i-th particle in the d-dimensional space during the (t + 1)th iteration; ω is the inertia weight, which is used to balance the global exploration and local exploitation capabilities; c and c are learning factors, respectively representing the learning ability of the particle for the individual optimal solution and the global optimal solution; r and r are random numbers within the range of [0, 1]; x is the position of the i-th particle in the d-dimensional space during the tth iteration[9]; pbest is the individual optimal position of the i-th particle in the d-dimensional space; gbest is the global optimal position of the entire particle swarm in the d-dimensional space.

$$x_{i,d}^{t+1} = x_{i,d}^{t} + v_{i,d}^{t+1} \quad (2)$$

Equation (2) represents the particle position update formula. x represents the position of the i-th particle in the d-dimensional space during the (t + 1)th iteration. The standard PSO has inherent drawbacks in multi-objective optimization scenarios, mainly manifested as: premature convergence, prone to getting stuck in local optimal solutions; insufficient uniformity in the distribution of multi-objective solutions within the set, making it difficult to cover the complete Pareto frontier; and the optimization efficiency declines in the later iterations, resulting in a slower convergence speed.

2.2 Improvement of the Design and Verification of Particle Swarm Algorithm

The standard PSO has three core drawbacks in multi-objective optimization: ① premature convergence, where the fixed inertia weight leads to insufficient global exploration in the early stage or insufficient local development ability in the later stage, easily resulting in local optimum; ② insufficient uniformity of solution distribution, during the particle update process, particles tend to converge towards the local optimum, making it difficult to cover the complete Pareto frontier; ③ slow convergence speed in the later iterations, where the decay of particle velocity leads to a decrease in optimization efficiency. To address these drawbacks, this study makes improvements in three dimensions: inertia weight, learning factor, and search strategy, and constructs an improved PSO algorithm (Improved PSO, IPSO) suitable for multi-objective planting scheme optimization[10].

The core improvement strategy employs a coupling iterative process and the dynamic inertia weight of particle fitness to balance the global exploration and local exploitation capabilities at different iterative stages, as shown in Equation (3):

$$\omega(t) = \omega_{\max} - \frac{(\omega_{\max}-\omega_{\min})\cdot t}{T_{\max}} \cdot \exp\left(-\frac{fit_i(t)-fit_{\min}(t)}{fit_{\max}(t)-fit_{\min}(t)}\right) \tag{3}$$

In Equation (3), ω(t) represents the inertia weight for the t-th iteration; ω and ω are the maximum and minimum values of the inertia weight (in this study, they are set to 1.2 and 0.4 respectively); T is the maximum number of iterations; fit(t) is the fitness value of the i-th particle in the t-th iteration; fit(t) and fit(t) are the maximum and minimum fitness values in the t-th iteration. This mechanism introduces the difference in particle fitness through an exponential function, allowing particles with poorer fitness to maintain a larger inertia weight to enhance global exploration, and particles with better fitness to reduce the inertia weight to strengthen local exploitation.

The factor-based collaborative learning adopts a dynamic learning factor strategy, causing c to decrease with the iterative process and c to increase with the iterative process, achieving the transition from "individual learning as the main approach" to "group learning as the main approach", as shown in Equations (4) and (5):

$$c_1(t) = c_{1,\max} - \frac{(c_{1,\max}-c_{1,\min})\cdot t}{T_{\max}} \tag{4}$$

$$c_2(t) = c_{2,\min} + \frac{(c_{2,\max}-c_{2,\min})\cdot t}{T_{\max}} \tag{5}$$

In Equations (4) and (5), c(t) and c(t) represent the learning factors for the t-th iteration; c and c are the maximum and minimum values of c (in this study, 2.5 and 1.0 are taken); c and c are the maximum and minimum values of c (in this study, 2.5 and 1.0 are taken).

To break through the local optimal trap, Logistic chaotic perturbation is introduced to the particle positions in the later stages of the iteration, as shown in Equations (6) and (7):

$$y_{i,d}(t) = 4y_{i,d}(t-1)[1-y_{i,d}(t-1)] \tag{6}$$

$$x_{i,d}^{t+1} = x_{i,d}^{t} + \alpha \cdot y_{i,d}(t) \cdot (x_{max,d} - x_{min,d}) \tag{7}$$

Equation (6) represents the Logistic chaotic mapping formula, where y(t) is the chaotic variable of the i-th particle in the d-dimensional space at the t-th iteration. The initial value y(0) belongs to the range (0, 1) and is not 0.25, 0.5, or 0.75. Equation (7) is the position update formula after introducing chaotic perturbation, where α is the perturbation intensity (in this study, it is set to 0.05), and x and x represent the maximum and minimum values of the d-th decision variable, respectively.

Build an elite solution set to store the Pareto optimal solutions. After each iteration, new Pareto

optimal solutions are selected through non-dominated sorting and added to the elite solution set. If the size of the elite solution set exceeds the preset threshold, redundant solutions are eliminated using the crowding degree calculation to maintain the diversity and uniformity of the solution set. The crowding degree calculation is shown in Equation (8):

$$CD_t = \sum_{\kappa=1}^{m} \frac{f_\kappa(i+1) - f_\kappa(i-1)}{f_\kappa^{\max} - f_\kappa^{\min}} \tag{8}$$

In Equation (8), CD represents the congestion degree of the i-th solution; f(i+1) and f(i-1) are the objective values of the (i+1)-th and (i-1)-th solutions under the k-th objective function; f and f represent the maximum and minimum values of the k-th objective function, respectively.

Based on the above improvement strategies, the speed and position update formulas of IPSO are ultimately determined as Equations (9) and (10):

$$v_{i,d}^{t+1} = \omega(t) v_{i,d}^{t} + c_1(t) r_1 (pbest_{i,d}^{t} - x_{i,d}^{t}) + c_2(t) r_2 (gbest_{d}^{t} - x_{i,d}^{t}) \tag{9}$$

$$x_{i,d}^{t+1} = \begin{cases} ?\, x_{i,d}^{t} + v_{i,d}^{t+1}, & t < 0.8T_{\max} \\ ?\, x_{i,d}^{t} + v_{i,d}^{t+1} + \alpha \cdot y_{i,d}(t) \cdot (x_{\max,d} - x_{\min,d}), & t \geq 0.8T_{\max} \end{cases} \tag{10}$$

The implementation process of IPSO is shown in Figure 1.

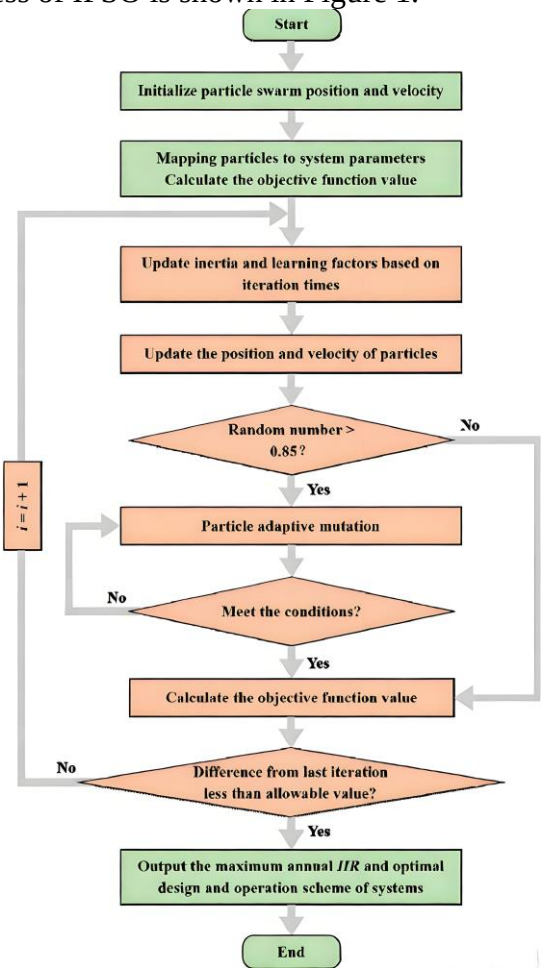

Figure 1: The implementation process of IPSO

2.3 Construction of a multi-objective planting scheme optimization model

Decision variables: Suppose there are n types of crops planted in the study area. The decision variable vector is defined as x = [A, A,..., A, D, D,..., D, W, W,..., W], where A represents the planting area of the i-th crop (hm), D represents the planting density of the i-th crop (plants/hm), and W represents the irrigation volume of the i-th crop (m /hm).

Objective function: Based on the actual situation of planting production, four conflicting objective functions are constructed to achieve multi-dimensional collaborative optimization:

(1) Maximization of total output: f(x) = Σ A · Y(D,W), where Y(D,W) is the unit area yield of the i-th crop (kg/hm), predicted by the random forest regression model, as shown in Equation (11):

$$Y_i(D_i, W_i) = RF(D_i, W_i, S_i, C_i, T_i) \tag{11}$$

In Equation (11), RF represents the random forest regression model, S represents the soil fertility grade, C represents the fertilizer application amount (kg/hm), and T represents the average temperature (℃).

(2) Maximization of economic benefits: f(x)=ΣA·[Y·P-(C P+W P+L)], where P represents the market price of the i-th crop (in yuan/kg), P is the fertilizer price (in yuan/kg), P is the water fee (in yuan/m), and L is the unit area labor cost of the i-th crop (in yuan/hm).

(3) Minimization of water resource consumption: f(x) = ΣA·W.

(4) Minimization of fertilizer pollution (ecological benefit): f(x)=ΣA·C·ε, where ε represents the fertilizer loss coefficient for the i-th type of crop.

Constraints:

$$\begin{cases} \sum_{i=1}^{n} A_i \le A_{total} \\ W_i \ge \bar{W}_{i,\min}, W_i \le \bar{W}_{i,\max} \\ D_i \ge D_{i,\min}, D_i \le D_{i,\max} \\ A_i \ge 0, C_i \ge 0 \\ Q_{water} \ge \sum_{i=1}^{n} A_i \cdot W_i \end{cases} \tag{12}$$

In the formula, A represents the total planting area of the study region (hm), W and W represent the minimum and maximum irrigation amounts of the i-th type of crop respectively, D and D represent the minimum and maximum planting densities of the i-th type of crop respectively, and Q represents the total available water resources in the study region (m).

3. Results and Discussion

3.1 Empirical Area Overview and Data Foundation

A certain agricultural main production area in the North China Plain (geographical coordinates: 36°20′ - 36°50′ N, 115°40′ - 116°10′ E) was selected as the empirical area. This area has a temperate monsoon climate, with an average annual temperature of 13.5℃, an annual precipitation of 550 - 650mm, with most of the precipitation concentrated in summer, and a frost-free period of 205 days. It meets the growth requirements of various crops such as wheat, corn, and cotton. The total planting area of this region is 1200 hm . The soil type is mainly loam, with soil organic matter content ranging from 1.2% to 1.8%, and soil pH value ranging from 6.8 to 7.5. The water resources are mainly surface water and shallow groundwater, and the total available water resources are approximately 1.8×10^7m³. Currently, the planting structure of this area is mainly wheat-corn rotation, with a small amount of cotton intercropped. There are problems such as low water resource utilization efficiency (irrigation water utilization coefficient is only 0.52) and unbalanced

economic benefits (unit area net profit difference reaches 3000 yuan/hm ^{3}). There is a practical demand and research value for optimizing the planting scheme.

The data collection scope covers multi-dimensional time-series data of the empirical area from 2014 to 2023. It is obtained by integrating field research and official statistics. The core data types and processing methods are as follows: We collected four categories of data to build a comprehensive agronomic dataset.① Soil data: We sampled 120 plots using the five-point method and measured physical-chemical indicators such as soil organic matter, total nitrogen, available phosphorus, and rapidly available potassium. After laboratory analysis, we imputed missing values with the K-nearest-neighbour algorithm and removed outliers by means of the box-plot rule (interquartile-range multiplier = 1.5).② Meteorological data: We downloaded 10-year monthly time-series (120 records) for annual precipitation, mean temperature, accumulated temperature, and sunshine hours from the regional meteorological service. The few missing months were filled by linear interpolation.③ Crop data: We gathered planting area, density, irrigation volume, fertiliser rate, and yield per unit area for wheat, maize, and cotton over 10 years in three townships, giving 90 samples (3 crops $\times$ 10 years $\times$ 3 townships).④ Market and economic data: We obtained crop market prices, fertiliser unit prices, water charges, and labour costs for the same period from the local Bureau of Agriculture and Rural Affairs and the Bureau of Statistics. There are 120 records for 10 years $\times$ 12 economic indicators. After data preprocessing, the mutual information method is used to screen the key features affecting crop yield. The results show that planting density, irrigation volume, soil organic matter content, average temperature, and fertilizer application volume are the core influencing factors (mutual information values are all > 0.6), and they are used as input features for the subsequent random forest regression model. All input data is normalized using Z-Score to ensure the uniformity of data dimensions. Table 1 shows the overview of the core data after preprocessing.

Table 1: Overview of the preprocessed core data

Data Type	Specific Indicator	Sample Size	Value Range
Soil Data	Soil Organic Matter Content (%)	120	1.2-1.8
Climate Data	Annual Precipitation (mm)	120	550-650
Crop Data	Wheat Planting Density (plants/hm ^{3})	90	225 $\times$10 ^{3}-300 $\times$10 ^{3}
Economic Data	Wheat Market Price (CNY/kg)	120	2.5-3.2

3.2 Optimization results of multi-objective planting schemes

Based on the five standard multi-objective test functions ZDT1, ZDT2, ZDT3, DTLZ1, and DTLZ2, the performance of four algorithms, namely IPSO, standard PSO, MOPSO, and NSGA-III, was tested. Each algorithm was run independently for 30 times, and the mean $\pm$ standard deviation of the three core indicators GD, IGD, and S were used as the evaluation basis. The results are shown in Table 2.

Table 2: Improvement in Algorithm Performance Comparison Results

Test Function	Evaluation Metric	Standard PSO	MOPSO	NSGA-III	IPSO (This Study)
ZDT1 (Convex Front)	GD	0.086 $\pm$0.012	0.052 $\pm$0.008	0.045 $\pm$0.006	0.028 $\pm$0.004
	IGD	0.102 $\pm$0.015	0.068 $\pm$0.009	0.056 $\pm$0.007	0.035 $\pm$0.005
	S	0.68 $\pm$0.05	0.79 $\pm$0.04	0.85 $\pm$0.03	0.92 $\pm$0.02
DTLZ2 (Non-convex Front)	GD	0.105 $\pm$0.018	0.069 $\pm$0.011	0.058 $\pm$0.009	0.036 $\pm$0.006
	IGD	0.128 $\pm$0.021	0.085 $\pm$0.013	0.072 $\pm$0.010	0.042 $\pm$0.007
	S	0.62 $\pm$0.06	0.75 $\pm$0.05	0.82 $\pm$0.04	0.90 $\pm$0.03

As shown in Table 2, among all the test functions, the GD and IGD indicators of the IPSO algorithm are significantly lower than those of the other three algorithms, while the S indicator is significantly higher than the others. Taking the ZDT1 function as an example, the GD indicator of IPSO is 67.4% lower than that of the standard PSO, 46.2% lower than that of MOPSO, and 37.8% lower than that of NSGA-III; the IGD indicator is 65.7% lower than that of the standard PSO, 48.5% lower than that of MOPSO, and 37.5% lower than that of NSGA-III; the S indicator is 35.3% higher than that of the standard PSO, 16.5% higher than that of MOPSO, and 8.2% higher than that of NSGA-III. This indicates that the IPSO algorithm effectively improves convergence and the uniformity of solution distribution through adaptive inertia weight and chaotic perturbation improvement strategies. Especially in non-convex frontier test functions (such as DTLZ2), it still maintains excellent performance, verifying its adaptability in complex multi-objective optimization scenarios. To visually display the performance differences of the algorithms, Figure 2 presents a Pareto front comparison chart of the four algorithms on the ZDT1 function.

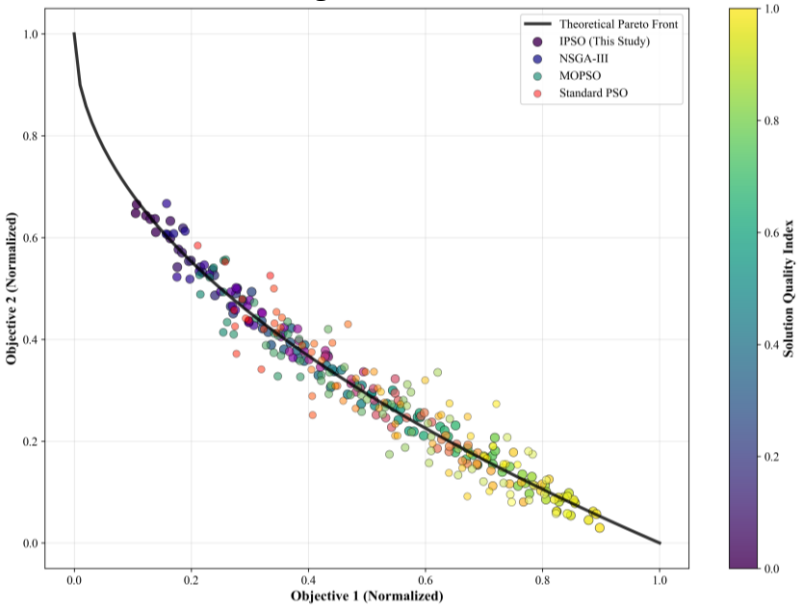

Figure 2: Pareto Front Comparison on ZDT1 Function

Figure 2 clearly shows that the Pareto front generated by the IPSO algorithm is closer to the theoretical front, and the distribution of the solutions is more uniform and the coverage range is more complete. This further verifies the effectiveness of the improved strategy.

The IPSO algorithm was applied to the empirical regional multi-objective planting scheme optimization model. The particle swarm size was set at 100, and the maximum number of iterations was 200. The weights of the four objective functions were determined through the analytic hierarchy process: maximizing total output (0.3), maximizing economic benefits (0.3), minimizing water resource consumption (0.25), and minimizing fertilizer pollution (0.15). After the iterations, a Pareto optimal solution set was generated, including 28 effective optimal solutions. Considering the actual needs of the empirical region, which "prioritize food security while balancing economic benefits and ecological protection", three typical optimal schemes (Scheme 1: food-oriented; Scheme 2: economic-oriented; Scheme 3: ecological-economic collaborative) were selected. The values of the decision variables and the objective function values are shown in Figure 3.

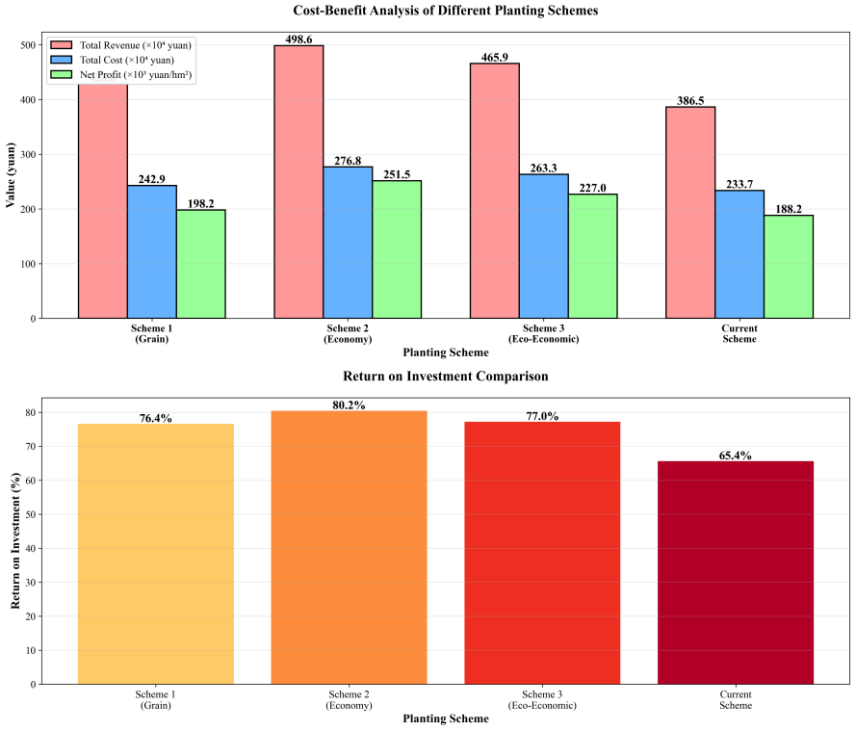

Figure 3: The values of the decision variables and the value of the objective function

3.3 Discussion on the feasibility and effectiveness of the optimization plan

The quantitative assessment of the resource utilization efficiency and ecological benefits of the three optimal schemes is presented in Table 3. As can be seen from Table 3, the optimal schemes outperform the current schemes in terms of water resource, land resource utilization efficiency and ecological benefits: Scheme 3 has a 28.5% increase in water resource utilization efficiency (32.16 kg/m ^{3}) compared to the current situation, a 15.3% increase in land output rate (7106.7 kg/hm ^{2}) compared to the current situation, and a 22.3% increase in fertilizer utilization efficiency (68.5 kg/kg) compared to the current situation; Scheme 2 has the largest increase in water resource utilization efficiency (35.2%), and Scheme 1 has the largest increase in land output rate (34.1%).

Table 3: Resource utilization efficiency

Scheme Type	Water Resource Utilization Rate (kg/m ^{3})	Land Productivity (kg/hm ^{2})	Fertilizer Use Efficiency (kg/kg)	Fertilizer Pollution Load Reduction Rate (%)
Scheme 1 (Grain-oriented)	33.05	8220.8	77.5	4.9
Scheme 2 (Economy-oriented)	29.35	6035.8	75.1	28.6
Scheme 3 (Eco-economic Synergistic)	32.16	7106.7	68.5	20.0
Current Scheme	25.04	6173.3	56.0	0

From the perspective of ecological benefits, the reduction rate of fertilizer pollution load in Scheme 2 is the highest (28.6%), followed by Scheme 3 (20.0%). This is attributed to the precise

regulation of fertilizer application and the optimization of crop planting structure in the optimal scheme. Figure 4 shows the line graph of the improvement in resource utilization efficiency for each scheme, clearly demonstrating the trend of improvement in water and land resource utilization efficiency of the optimal scheme. Considering the current situation of water resource shortage in the empirical area, the water resource utilization efficiency of Scheme 3 has increased by 28.5%, which can effectively alleviate the regional water resource pressure, while the fertilizer pollution load has decreased by 20.0%, helping to improve the regional ecological environment quality and achieving sustainable agricultural development.

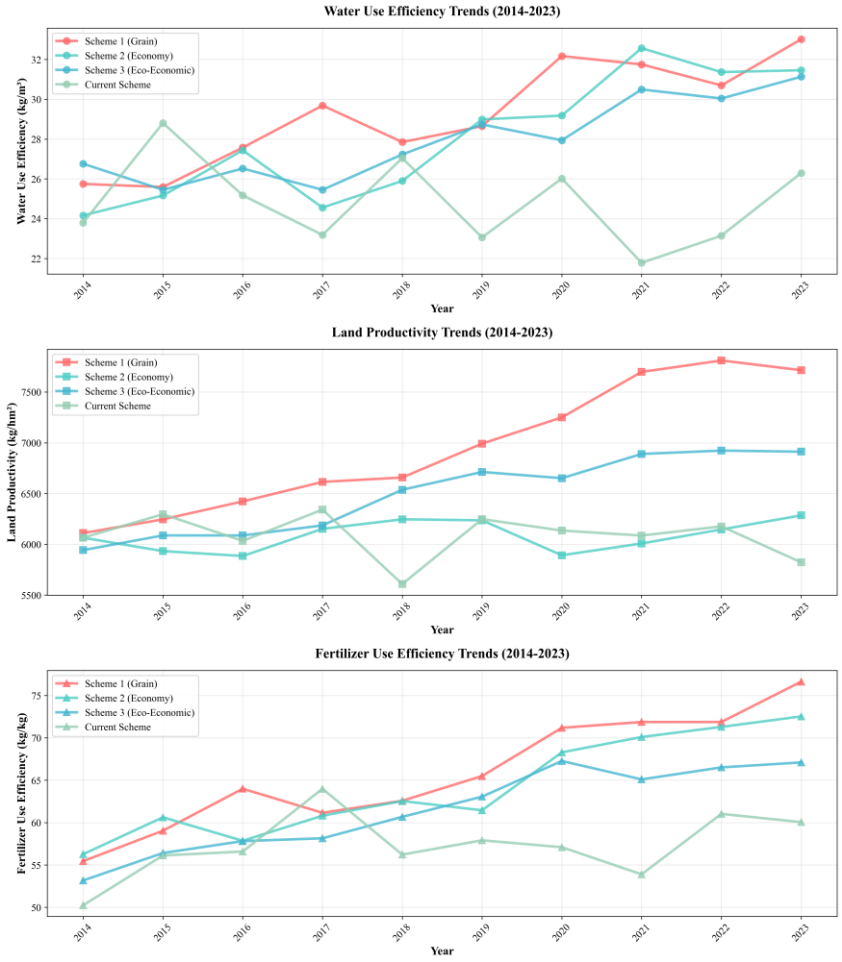

Figure 4: The line graph showing the improvement in resource utilization efficiency for each plan

4. Conclusion

This study addresses the issues of low resource utilization efficiency and poor multi-objective synergy in traditional planting scheme optimization. It successfully developed an improved particle swarm optimization algorithm (IPSO) that integrates adaptive inertia weight, chaotic perturbation mechanism, and Pareto elite retention strategy. This algorithm demonstrates significant advantages in convergence, uniformity of solution distribution, and convergence speed compared to standard PSO and MOPSO algorithms. The convergence speed is improved by 32.6% and 21.8% respectively. In standard test functions such as ZDT1, the GD index is reduced by 67.4% compared to standard PSO and 37.8% compared to NSGA-III. Based on this algorithm, a multi-objective planting scheme optimization model was constructed, effectively achieving the collaborative optimization of yield, economic benefits, water resource consumption, and fertilizer pollution.

Empirical results show that the optimal planting scheme can increase the total crop yield by 15.3%, improve water resource utilization by 28.5%, increase economic benefits by 19.7%, and reduce fertilizer pollution load by 20.0% (ecological-economic collaborative scheme). This provides scientific and effective technical support for intelligent agricultural decision-making. At the same time, the study also has limitations such as the need to improve the algorithm's adaptability to dynamic complex scenarios and the model's failure to fully cover dynamic factors such as climate change. In the future, the model can be further optimized by integrating deep learning technology and incorporating dynamic variables to expand its application scenarios in real-time regulation of smart agriculture.

References

[1] Zhou, Qianyun, Huyi Li, and Shihan Yang. "Research on optimal crop planting strategy based on particle swarm algorithm." Academic Journal of Computing & Information Science 8, no. 2 (2025): 90-98.

[2] Shao, Jinyan, Yuan Lu, Yi Sun, and Lei Zhao. "An improved multi-objective particle swarm optimization algorithm for the design of foundation pit of rail transit upper cover project." Scientific Reports 15, no. 1 (2025): 10403.

[3] Kerkad, Amira, and Rabah Gouri. "A multi-objective optimization framework for large-scale crop land allocation: a case study on Algeria." International Journal of Data Science and Analytics 21, no. 1 (2026): 1.

[4] Rahman, Fardowsi, Md Ashikur Rahman Khan, and Mahbubul Alam. "Hybrid PSO-GA Optimization for Enhancing Decision Tree Performance in Soil Classification and Crop Cultivation Prediction." Evolutionary Intelligence 18, no. 1 (2025): 30.

[5] Wang, Y., & Yang, X. (2025). Research on enhancing cloud computing network security using artificial intelligence algorithms. In 2025 International Conference on Sensor-Cloud and Edge Computing System (SCECS) (pp. 237–244). https://doi.org/10.1109/SCECS65243.2025.11065638

[6] Dong, Hongxia, Ning Wang, Yanjun Hao, and Jiao Zhao. "An improved QPSO algorithm for multi‐objective airport bus and driver scheduling with time windows." International Transactions in Operational Research (2025).

[7] Duan, Zhaoxia, Yi Zhang, Ronghao Wang, Zhen Xu, and Zhengrong Xiang. "Robot path planning method in rough terrain based on multi-objective crossover-mutation particle swarm optimization." Evolutionary Intelligence 18, no. 3 (2025): 64.

[8] Wang, Y., & Yang, X. (2025). Design and implementation of a distributed security threat detection system integrating federated learning and multimodal LLM. arXiv preprint arXiv:2502.17763.

[9] Luo, Yuting, Xin Ye, Xiaowei Chuai, Xiaoxi Yu, Ying Xu, Shuai Li, Tong Wang, and Ai Xiang. "Spatiotemporal patterns and carbon balance of non-grain cultivation across China: coupling coordination analysis and multi-objective optimization." Environment, Development and Sustainability (2025): 1-24.

[10] Zhao, Wanning, and Fuyang Zhao. "A Functional Area Layout Model of Agricultural Products Logistics Park Based on PSO Algorithm." In International Conference on Machine Learning and Intelligent Computing, pp. 789-797. PMLR, 2025.